

Article

Development of Kraft Lignin Chemically Modified as a Novel Crosslinking Agent for the Synthesis of Active Hydrogels

Diana Rico-García ¹, Luis Guillermo Guerrero-Ramírez ¹, Leonardo Ramses Cajero-Zul ² ,
Euologio Orozco-Guareño ¹, Edgar Benjamin Figueroa-Ochoa ¹ , Ramon Alejandro Gutiérrez-Saucedo ¹,
Leyre Perez-Alvarez ³ , Jose Luis Vilas-Vilela ³  and Saira Lizette Hernandez-Olmos ^{1,*}

- ¹ Chemistry Department, University Center of Exact Sciences and Engineering, University of Guadalajara, 44430 Guadalajara, Mexico; diana.rico3332@alumnos.udg.mx (D.R.-G.); lguillermo.guerrero@academicos.udg.mx (L.G.G.-R.); euologio.orozco@academicos.udg.mx (E.O.-G.); benjamin.figueroa@academicos.udg.mx (E.B.F.-O.); ramon.gsaucedo@academicos.udg.mx (R.A.G.-S.)
- ² Chemical Engineering Department, University Center of Exact Sciences and Engineering, University of Guadalajara, 44430 Guadalajara, Mexico; leonardo.cajero@academicos.udg.mx
- ³ Macromolecular Chemistry Group, Physics and Chemistry Department, Science and Technology Faculty, University of Basque Country, 48940 Leioa, Spain; leyre.perez@ehu.eus (L.P.-A.); joseluis.vilas@ehu.es (J.L.V.-V.)
- * Correspondence: saira.hernandez@academicos.udg.mx



Citation: Rico-García, D.; Guerrero-Ramírez, L.G.; Cajero-Zul, L.R.; Orozco-Guareño, E.; Figueroa-Ochoa, E.B.; Gutiérrez-Saucedo, R.A.; Perez-Alvarez, L.; Vilas-Vilela, J.L.; Hernandez-Olmos, S.L. Development of Kraft Lignin Chemically Modified as a Novel Crosslinking Agent for the Synthesis of Active Hydrogels. *Appl. Sci.* **2021**, *11*, 4012. <https://doi.org/10.3390/app11094012>

Academic Editor: Rafal Malinowski

Received: 22 March 2021

Accepted: 24 April 2021

Published: 28 April 2021

Publisher's Note: MDPI stays neutral with regard to jurisdictional claims in published maps and institutional affiliations.



Copyright: © 2021 by the authors. Licensee MDPI, Basel, Switzerland. This article is an open access article distributed under the terms and conditions of the Creative Commons Attribution (CC BY) license (<https://creativecommons.org/licenses/by/4.0/>).

Abstract: In this research a chemical modification of kraft lignin was carried out using a basic nucleophilic substitution reaction (NS_A) in order to functionalize it as a novel crosslinking agent for the synthesis of active hydrogels. The chemical modification success of the synthesized crosslinker was demonstrated by using several techniques such as volumetry probes, FTIR, 1H -NMR and DSC. Thus, the obtained materials were employed during the synthesis of acrylic acid-based hydrogels, due to its high-water absorption capacity to evaluate their retention potential of heavy metal ions. Characterization of the active hydrogels were performed by FTIR and SEM, showing the specific signals corresponding to the base monomers into the polymer skeleton and the efficiency of modified kraft lignin as a novel crosslinking agent. Additionally, to demonstrate the potential use of these hydrogels in wastewater treatment, metal ions adsorption experiments were conducted, showing adsorption percentages higher than 90% and 80% for Pb^{2+} and Cu^{2+} , respectively.

Keywords: novel crosslinking; active hydrogels; adsorption experiments

1. Introduction

Nowadays, the problem of water pollution is one of the most worrying aspects of the degradation of the natural environment, being considered a universal problem [1]. The different studies on wastewater indicate that pollution has, among other causes, an anthropogenic origin, where the main pollutants are pesticides, hydrocarbons and heavy metals. Metals can come from both urban effluents (food, pharmaceuticals, cosmetics, cleaning products, etc.), and from industrial sources (paper industries, paints, pigments, and coatings, etc.) [2].

Considering the high toxicity of heavy metals and the damage they can cause in biological systems, there is a great need for their removal from aqueous effluents, which can be carried out using different treatments [3,4].

The most common processes involve precipitation by hydroxides or sulfides, oxidation-reduction, ion exchange, solid-liquid separation by decantation-flotation and separation by membranes [5]. Unfortunately, these techniques have limited application due to different factors.

A great alternative is the use of polymeric materials. Specifically, the use of hydrogels as adsorption materials for toxic metal ions present in aqueous solutions has recently

increased [6–9], becoming one of the conventional methods and techniques for environmental decontamination, due to the following advantages: (a) they can be reusable materials, showing good results during several adsorption and desorption cycles [10], and, (b) present low cost and low toxicity.

Owing to the presence of big functional groups in its structure, in recent years the studies about the practical utility of the lignin have been increased, finding that it may be used in adhesive formulations. The lignin is a natural complex macromolecule that can be found in most of the land vascular plants [11]. However, the patterns and distributions of its functional groups are not precise nowadays, which bestows it a big structural complexity and heterogeneity. The lignin has a well known biodegradability properties and due this [12,13], its use is widely approach for different purposes, but still is not explored the manipulation of its functional groups to generate a chemically modified lignin in order to use it as a crosslinking monomer (crosslinking agent) [14] in the synthesis of polymeric hydrogels.

Currently, other organic compounds such as ginipin, tannic acid and citric acid have been used as crosslinking agents in the synthesis of hydrogels based on chitosan [15], hydroxyethylcellulose [16], xanthan [17], carboxymethylcellulose [18] and other monomers [19]. However, these organic crosslinking agents were used in polycondensation reactions showing a significant restriction like slow polymerization velocity and endothermic reactions in hydrogel's synthesis.

On the other hand, the hydrogels obtained by chemical crosslinking are polymeric materials of natural or synthetic origin with tridimensional network shapes [20]. They are obtained through the simultaneous polymerization and crosslinking of one or many polyfunctional monomers. In many of the cases, only one monomer provides well mechanical properties and big water retention, so it is necessary to resort to copolymerization [21] in order to be able to obtain a better performance of these properties. The hydrogels stand out owing to their swelling, morphology and resistance properties to the compression based on their chemical composition and synthesis condition [22].

Other interesting properties of these materials are their capacity to control the diffusion process [23], their answer to the ionic strength changes, pH [24], temperature [25] and the capacity for catching the chemical species through the polar functional groups that interact in a selective way and strongly with these species [26].

As far as relates to the swelling, the elemental difference among crisscross and non-crisscross polymers is that the liquid entrance cannot be separated because they are connected in a covalent way [27]. Otherwise, the non-crisscrossed polymers, when the liquid proportion increases, the elastic solid aspect shall change to the viscous liquid aspect, not being able to support its shape, which for some cases it can reduce its application [28].

In order to approach the lignin effectiveness on removing metallic ions, Peñaranda and collaborators (2010), synthesized acrylamide/lignin interpenetrating network hydrogels (IPN) and they were used for removing Cu (II) and Ni (II) using different pH values. These authors determined that the optimum pH value of metals sorption was 5.5, achieving removal capacities superior to 60% using only 0.1% of lignin [29]. In spite of, the use of lignin in the synthesis of IPN hydrogels has a restriction in the amount of lignin that can be used due to the size of it [28].

In this study, the characterization for both modified lignin and modified lignin crosslinked hydrogels have been obtained by Fourier transform infrared spectroscopy (FTIR), differential scanning calorimetry (DSC), nuclear magnetic resonance ($^1\text{H-NMR}$) and scanning electron microscopy (SEM) to demonstrate the success of the synthetic procedure.

2. Experimental

2.1. Materials

In the development of this work alkali kraft lignin (AKL) with 95% purity, acryloyl chloride with 97% purity, tetrahydrofuran (THF) with 99.9% purity, double-distilled water (MilliQ quality), acrylic acid 99% purity, *N,N*-methylenebisacrylamide (NMBA) 99% purity,

sodium bisulfite 99.5% purity, potassium persulfate 99% purity and copper sulfate pentahydrate $\text{CuSO}_4 \cdot 5\text{H}_2\text{O}$ with 99% purity were used; all these reagents were supplied by Sigma Aldrich (San Luis, MO, USA). Another reagent used, lead nitrate $[\text{Pb}(\text{NO}_3)_2]$ with 99% purity, was provided by J.T Baker (Madrid, Spain).

2.2. Characterization Techniques

2.2.1. Differential Scanning Calorimetry (DSC)

Thermograms were obtained using a differential scanning calorimeter Q-100 from TA Instruments (New Castle, DE, USA), that was previously calibrated with indium and sapphire, for temperature and heat capacity, respectively. The temperature range measured was from -70 to 250 °C with a heating ramp of 20 °C/min and cooling rates according to the standard procedures provided by TA Instruments equipment. Aluminum pans for volatile samples were employed to minimize losses by evaporation. Transition temperatures where the baseline changed slope significantly by the midpoint criterion.

2.2.2. Fourier Transformed Infrared Spectroscopy (FTIR)

FTIR spectra were collected using an iS50 Fourier Transformed Infrared Spectrometer (FTIR, Nicolet, Waltham, MA, USA) in a wavenumber range of 400 to 4000 cm^{-1} with a resolution of 4 cm^{-1} . All spectra were obtained on an average of 100 scans with a baseline correction and maximum peak detection to get an accurate qualitative measurement of the general and specific vibrations of principal functional groups. The sample was dried in an oven at 50 °C for 48 h. Then a portion of 0.5 g was placed on the ATR accessory coupled to the FTIR equipment prior to the data collection.

2.2.3. ^1H -NMR

All NMR spectra were recorded on an AV 500 MHz spectrometer (Bruker, Billerica, MA, USA) equipped with a 5 mm BBI probe and gradients on the Z axis at 25 °C. For ^1H -NMR analysis 30 mg of kraft lignin was dissolved in 1 mL of deuterated water (D_2O). Data acquisition and processing was carried out with TOPSPIN 1.3 (Bruker) software. The pulse sequences used were the Bruker standard ones. The peak (4.5 ppm) of D_2O was used as an internal reference.

2.2.4. Conductivity

Samples of AKL and modified AKL were prepared at 50 ppm for this analysis. Aliquots of 10 mL were taken and raised to 40 °C. Simultaneously a NaOH 0.01 N solution was placed on a burette and then added in volumes of 0.2 mL to measure conductivity with a Star A211 pH Meter (Orion, Waltham, MA, USA). The titration curve obtained was employed to determine the equivalent volume by the slope change using the midpoint criterion; additionally, the first derivative was calculated to increase the accuracy in the measurement.

2.2.5. FE-SEM

Hydrogel discs previously swollen in water were frozen. Then they were then fragmented into small pieces to observe the internal morphology of the hydrogels during the FE-SEM analysis. To eliminate the frozen water inside the swollen hydrogels, a lyophilizer was used, and the weight was monitored until it was constant. The fragments obtained were coated with gold using an ionic coating system. Finally, the morphology of the hydrogels was studied using a TESCAN (Brno, Czech Republic) brand field emission electron microscope with an accelerating voltage of 10 kV and different levels of magnification.

2.2.6. Atomic Absorption

All copper (Cu^{+2}) and lead (Pb^{+2}) ions quantification experiments were measured by the flame atomic absorption technique. The used spectrometer was an ContrAA 300 model (Analytik Jena, Jena, Germany) equipped with a High-Resolution Continuum Source

AAS (HR-CS AAS). Each sample was measured under conditions of primary wavelength by triplicate.

2.3. Methods

2.3.1. Alkali Kraft Lignin Chemical Modification

Required amount of alkali kraft lignin (AKL) was diluted in double distilled water and placed in a bath at $-5\text{ }^{\circ}\text{C}$, prior to the chemical modification of AKL, the prepared solution was kept under continuous stirring and then acryloyl chloride was drop by drop added. Once the NS reaction took place the reaction mixture was retired from the ice-water medium and THF was added to precipitate modified AKL and then poured and dried in a stove at $50\text{ }^{\circ}\text{C}$ for 24 h to obtain pure modified AKL.

2.3.2. Hydrogel's Synthesis and Swelling Probes

The synthesis of hydrogels was carried out by dispersing the specific amounts (mass ratios can be found in Table 1) of doubly distilled water, acrylic acid, modified AKL and NMBA, under nitrogen bubbling for 20 min prior to beginning the reaction. Then sodium bisulfite and potassium persulfate (previously both diluted in doubly distilled water) were added and let polymerize. After the polymerization was carried out, the reaction mixture was retired from the vial and washed with doubly distilled water. After polymerization, hydrogels were cut in discs and let dry in order to carry out the swelling test. For carrying out the swelling test, the xerogel (dry hydrogel) was placed in doubly distilled water and weighed from time to time until the weight of swell hydrogel was able to be constant.

Table 1. Mass ratios of synthesized hydrogels of AA/modified AKL.

Sample ID	AA/Modified AKL/Crosslinker	Sample ID	AA/Modified AKL/Crosslinker
AALm4	96/4/0%	AALm7nM0.1	92.9/7/0.1%
AALm5	95/5/0%	AALm7nM0.2	92.8/7/0.2%
AALm6	94/6/0%	AALm7nM0.3	92.7/7/0.3%
AALm7	93/7/0%	AALm7nM0.4	92.6/7/0.4%
AALm8	92/8/0%	AALm7nM0.5	92.5/7/0.5%

2.3.3. Water Absorption of the Hydrogels

The swelling kinetics in water was studied through a gravimetric technique. For obtaining the swelling percentage in function of the contact time, the xerogel was previously weighed and submerged in a container with doubly distilled water with a temperature of $25\text{ }^{\circ}\text{C}$, later the hydrogel was weighed from time to time drying it with an absorbent paper to remove the excess of water on the surface. The swelling percentage for each sample was calculated through a mass balance, which can be represented in the following equation:

$$\% \text{ of swelling} = \left[\frac{W - W_0}{W_0} \right] * (100)$$

where W = Hydrogel weight as time function (g) and W_0 = Xerogel weight (g).

2.3.4. Metal Ion Adsorption

The experimental conditions followed in order to carry out the maximum adsorption test of Pb^{2+} and Cu^{2+} were a two steps way: in a separately route, lead and cooper solutions were prepared with concentrations of 30 mg/L (valued through atomic abortion, with a real concentration of 30.3 ppm and 30.6 ppm, respectively) from lead nitrate $\text{Pb}(\text{NO}_3)_2$ and cooper sulfate pentahydrate $\text{CuSO}_4 \cdot 5\text{H}_2\text{O}$. The pH was determined, and the solutions were adjusted at values of 2, 4, 5 and 5.5 using an aqueous solution of NaOH and HNO_3 . Subsequently, samples of xerogel were weighed and were placed in Erlenmeyer flasks; then a control volume of lead and cooper solution was added to each flask separately. The flask

was placed in a stirring plate to 120 rpm and room temperature of 25 °C. After stirring solutions for 4 h, the sample was filtered using a filter paper with a pore number size of 40 micrometers to dry the hydrogel and let the lead and copper residuary quantity in the final solution¹⁸. The percent removal values were calculated from the change in solution concentration using the following equation:

$$\text{Percent removal} = \frac{(M)_0 - (M)_{eq}}{(M)_0} * 100$$

where $(M)_0$ = Initial metal concentration in the solution (mg/L) and $(M)_{eq}$ = Remaining metal concentration in the solution (mg/L)

3. Results

3.1. Kraft Lignin Functionalization

3.1.1. Conductivity Test of AKL

Figure 1 shows the obtained values for the AKL and modified AKL conductivity in the titration process. In this figure can be observed that the conductivity of both samples decreases as the volume of 0.01 N NaOH solution increases, being in the whole experiment the values of the conductivity for the functionalized AKL higher than AKL. On the other hand, functionalized AKL requires an equivalent volume of 0.8 mL of solution, whereas for AKL only 1.0 mL is required. The decrease in the equivalent volume in both samples is indicative that a 20% of chemical modification was performed in the process.

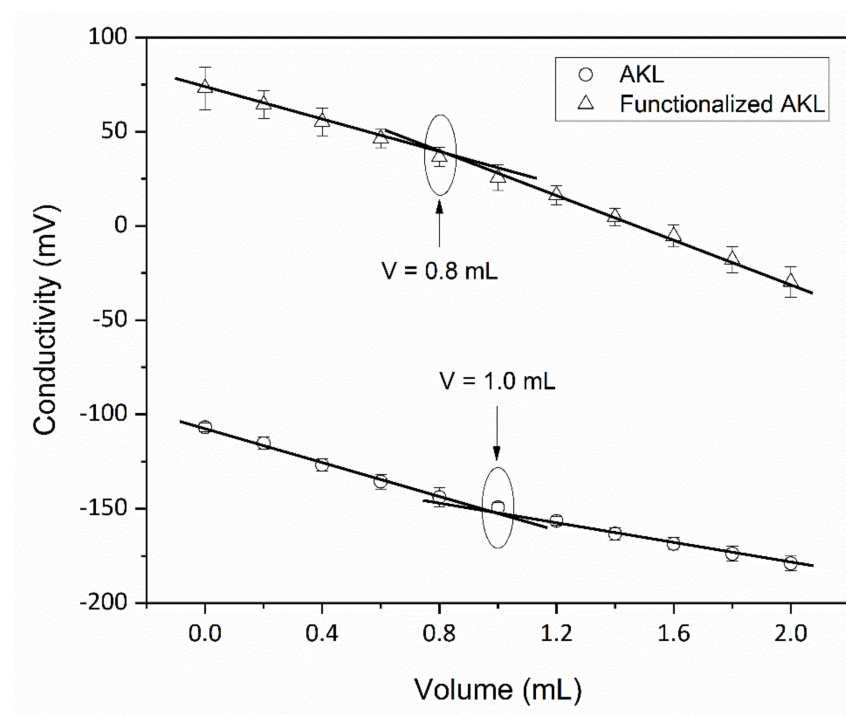


Figure 1. Measurement of conductivity of the AKL and functionalized AKL.

3.1.2. FTIR of AKL

In Figure 2 the obtained spectra for AKL and modified AKL are presented. In this figure the principal vibrations bands for AKL located at 3400 cm^{-1} corresponding to the bending vibration of the -OH functional group, 1600 cm^{-1} generated by the stretching vibration of the ether functional groups attached to the AKL can be appreciated [30]. On the other hand, in the functionalized AKL spectrum the -OH bending vibration presents a decrease in intensity that suggests a partial reaction of the total population of -OH functional groups, while a new signal appears at 1713 cm^{-1} originated by the vinyl-ester

group formed during the NS_A reaction, according to Scheme 1. In addition, the decrease of the stretching vibration of the ether functional groups indicates a secondary reaction where R-O-R' acts as a nucleophile in the same reaction. This type of reaction using acryloyl chloride in aqueous medium has been reported by other authors [31–33].

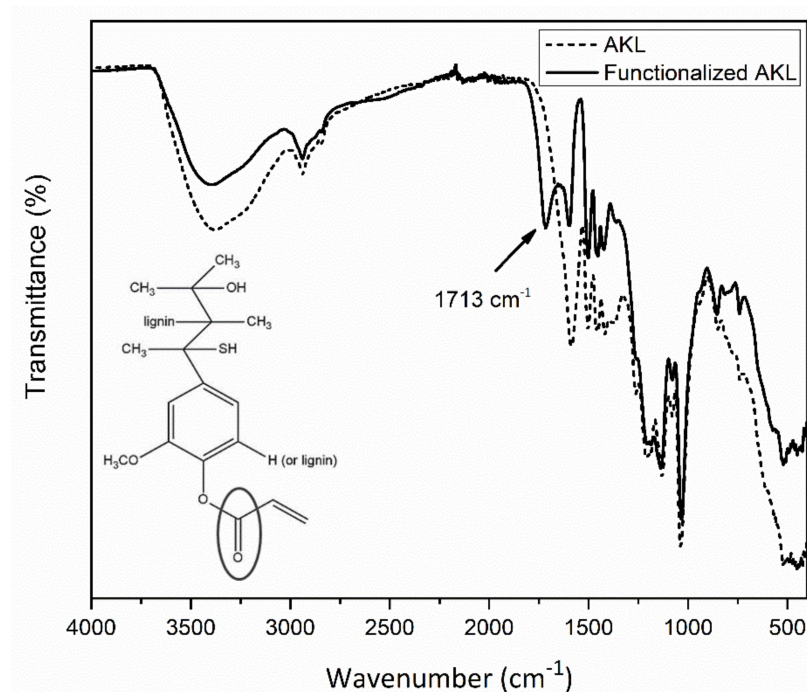
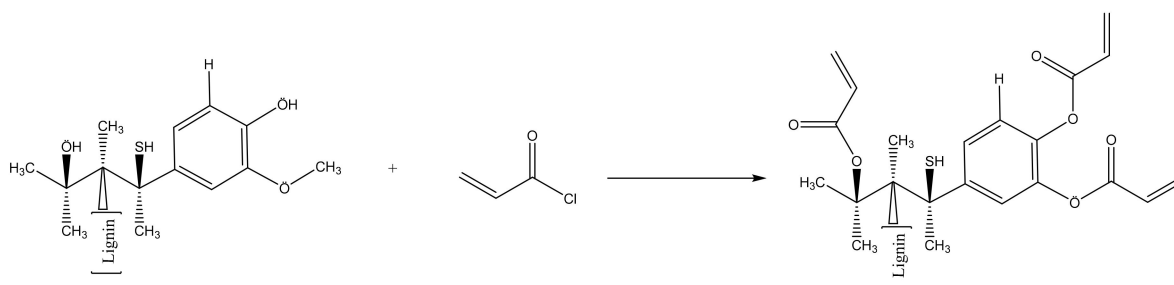


Figure 2. FTIR analysis of the AKL (dash line) and functionalized AKL (straight line).



Scheme 1. Reaction for acryloyl chloride in the presence of AKL.

3.1.3. ¹H-NMR of AKL

In Figure 3 it can be observed that the chemical shifts in the spectrum (A) faithfully correspond to the signals generated by the vinyl protons (H₁ and H₂) from the acryloyl chloride. On the other hand, in the AKL spectrum (B) these signals are absent because the functional groups there are related to the -OH and -C=O groups located within their structure; the signals of 0.7, 1.2, 1.7 and 3.7 ppm, correspond to the appearance of the protons from the -CH₃ and -R-O-CH₃ groups [34]. Also, in the spectrum (C) the signals corresponding to 5.3, 6 and 6.3 ppm demonstrate that new vinyl groups were incorporated into the structure of the AKL, where the separation of these signals is substantially different from those presented by the acryloyl chloride. The success in the chemical modification of the AKL can be confirmed by these signals; this difference can be attributed to the fact that the coupling constants (*J*) of the vinyl protons in the functionalized AKL have higher values respect to those presented by the acryloyl chloride, produced by the change in the chemical environment of AKL functional groups.

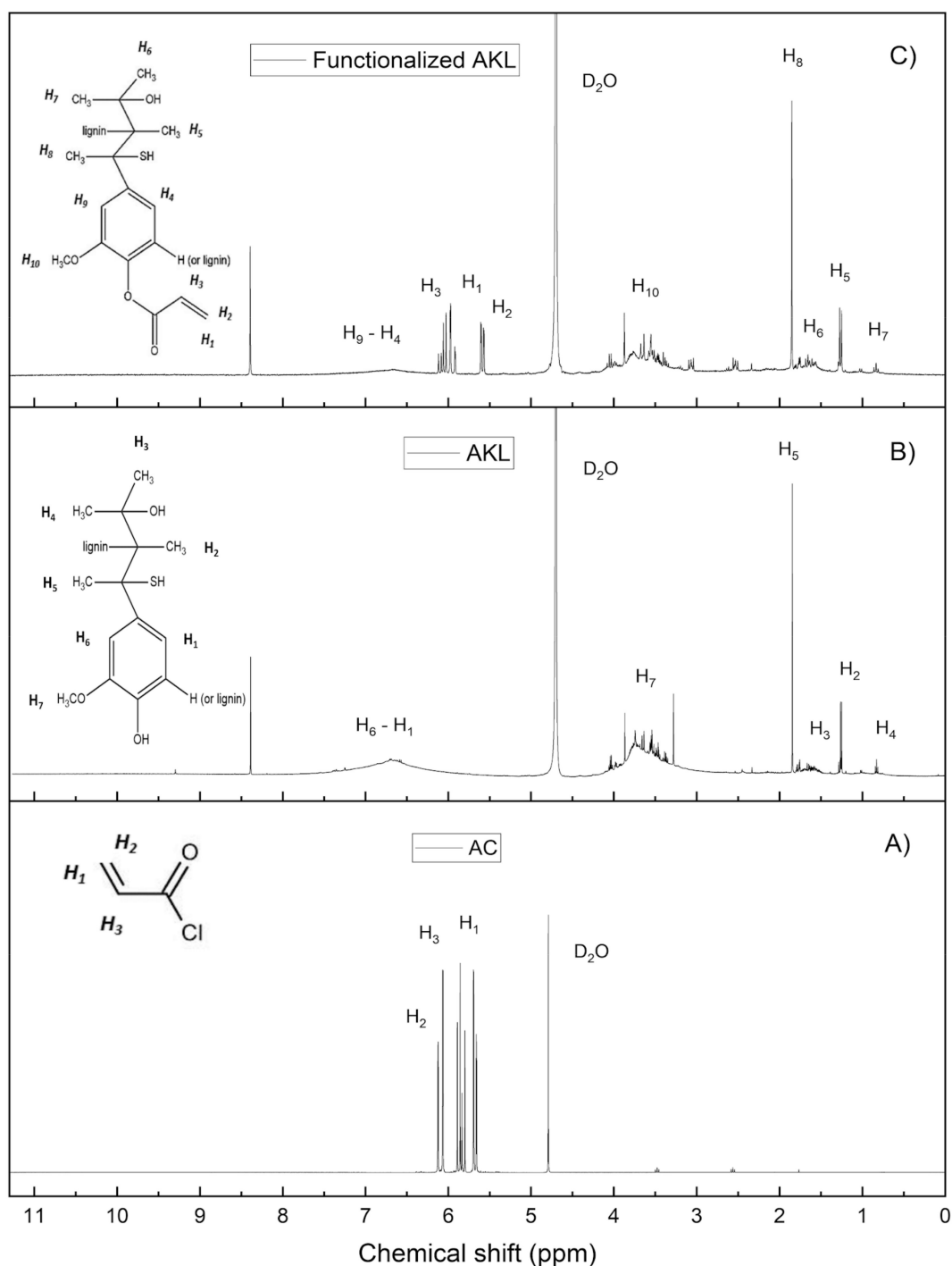


Figure 3. ^1H NMR analysis of acryloyl chloride (A), AKL (B) and functionalized AKL (C).

3.1.4. DSC of AKL

The DCS analysis of samples of AKL and functionalized AKL are shown in Figure 4. In the AKL thermogram a glass transition temperature (T_g) appears at 74°C ; AKL usually shows T_g above 90°C [35]. Nevertheless, there is reported data that specifies that high-purity, low molecular weight and functionality presents a lower glass transition temperature [36] which indicates the possibility in this case. Also, the thermogram of functionalized AKL shows a T_g at 78°C , this gain of 4°C in T_g is associated with the functionalization treatment of AKL.

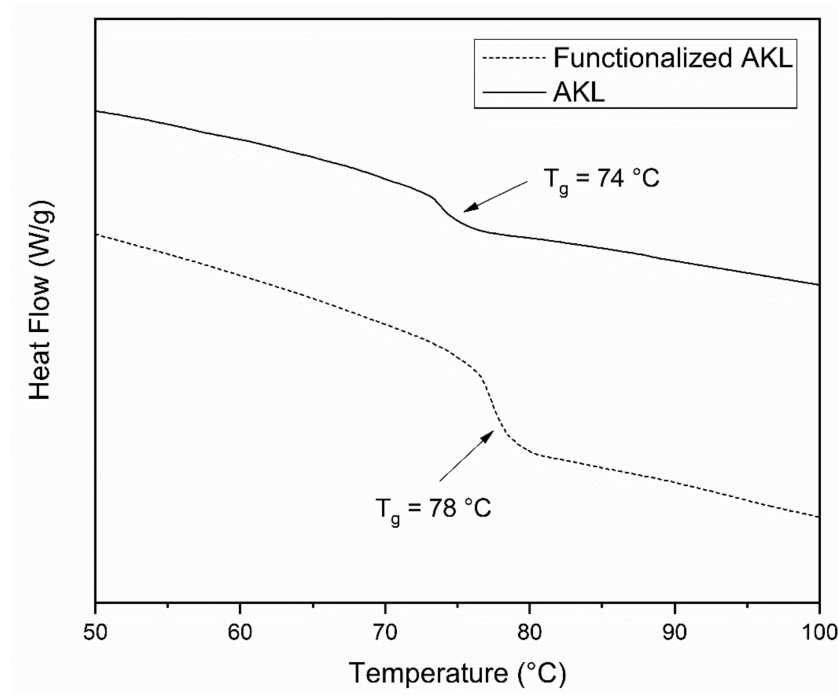


Figure 4. DSC thermograms for functionalized AKL (dash line) and AKL (straight line).

3.2. Hydrogels Synthesis

3.2.1. FE-SEM of Hydrogels

The water-swollen hydrogel AALm7 formulation was observed by SEM to study its morphology features like the type of surface it shows and the average pore size it shows. SEM analysis showed a homogeneous morphology with a continuous cutting surface and drop-shaped pores which have an average diameter of 25–50 μm . The SEM micrographs of hydrogels obtained are consistent with the SEM images obtained by Ji, X. et al. in 2017, which material reports surfaces of the hydrogel have many irregular pores with sizes of several micrometers to tens of micrometers (Figure 5). The hydrogels with different amounts of lignin were similar in structure, where they synthesized and characterized hydrogels based on alkaline lignin from ionic liquids [37].

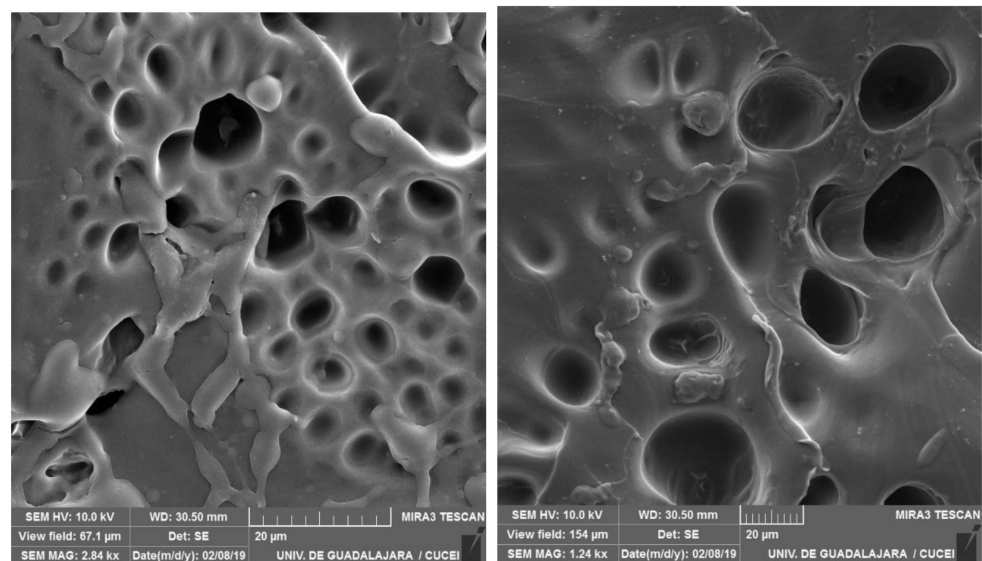


Figure 5. Scanning electron microscopy image of hydrogel swelling AALm7.

3.2.2. FTIR of Hydrogels

Figure 6 shows the FTIR analysis of a hydrogel sample with 7% of functionalized AKL and without. To substitute the effect of cross-linked and formed hydrogel, *N,N*-methylenebisacrylamide (NMBA) was added to the sample which does not have AKL. Both spectra show a great similarity, the only difference appearing at 1535 cm^{-1} that corresponds to the amide functional group on the cross-linked *N,N*-methylenebisacrylamide groups of the hydrogel. This means that the addition of AKL creates a good cross-linked structure and can be a good substitute of NMBA, which has been reported to be a harmful substance to cells and microorganisms [38].

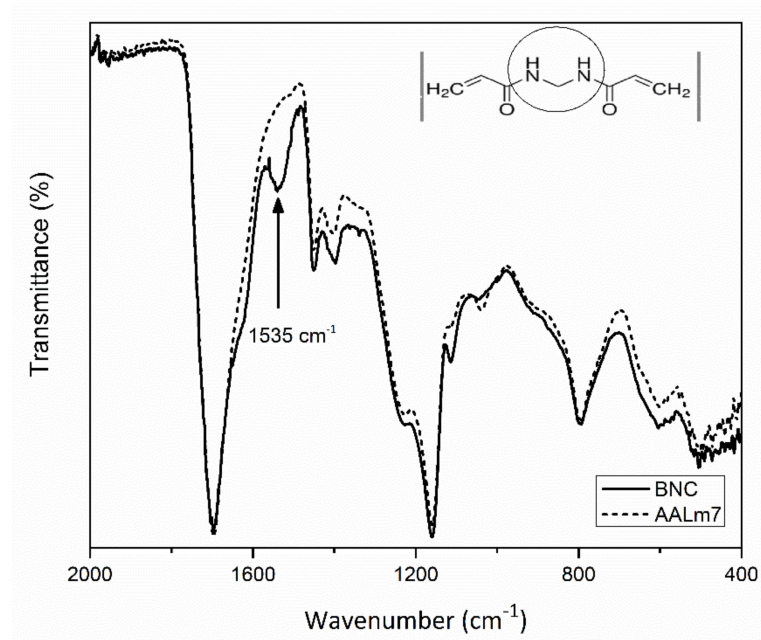


Figure 6. FTIR analysis of samples of BNC (straight line) and AALm7 (dash line) hydrogels.

The spectrum of AALm7, corresponds to the sample of hydrogel with modified lignin. It shows a spectral contribution at 1100 cm^{-1} that corresponds to thiol (R-SH) functionality of the kraft lignin used in the hydrogel synthesis.

3.2.3. Water Absorption of the Hydrogels

When the hydrogels of each formulation were exposed to a water absorption process, their dimensions and weight increased over time, showing that they were indeed swollen. At the end of the tests, the samples of all the formulations maintained their shape (cylinders) and their dimensional stability. However, the formulation gels containing only functionalized AKL and AA showed some degree of fragility in their swollen state against the formulations of NMBA, AA and functionalized AKL.

It is known that the swelling of the hydrogels demonstrates the degree of cross-linking that the gels have reached due to the chemical nature of their components and the degree of cross-linking of each formulation. Therefore, low percentages of swelling are obtained by those samples whose structure is sufficiently reticulated, considerably limiting the mobility of their chain, making the gels more rigid and, therefore, making it difficult to diffuse the water through the network. Likewise, the samples that show high percentages of swelling have a more flexible network structure and a lower reticulation density, which allows greater mobility of the chain due to a lower number of anchorage points between them [39]. Figure 7 shows the maximum values of water absorption and swelling for each formulation of hydrogels with functionalized AKL and AA. In this figure it can be clearly seen that swelling percentages change significantly by changing the concentration of functionalized

AKL in the formulations, thus demonstrating that the functionalized AKL is working as a crosslinker in these hydrogels.

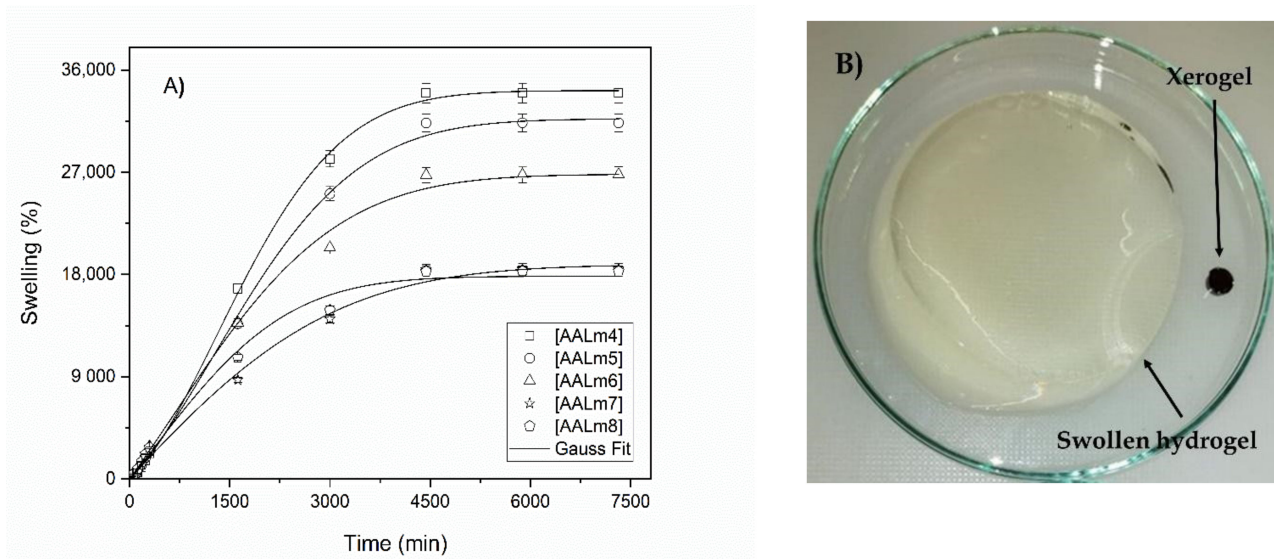


Figure 7. Swelling in water of hydrogels with AA and functionalized AKL. (A) Swelling behavior of hydrogels, (B) comparative capture of xerogel and swollen hydrogel.

According to Figure 7, the formulation gel AALm4 showed the highest percentage of swelling when reaching 35,000% swelling. This formulation is the one that contains a lower concentration of functionalized AKL, therefore, these swelling results coincide with the abovementioned ones. Otherwise, Figure 8 shows the swelling percentage graph of the formulations containing, in addition to functionalized AKL, NMBA as a crosslinker. In this graph it is again observed that the formulation AALm7nM0.1 with the lowest amount of crosslinker in its formation is the one with the highest swelling percentage.

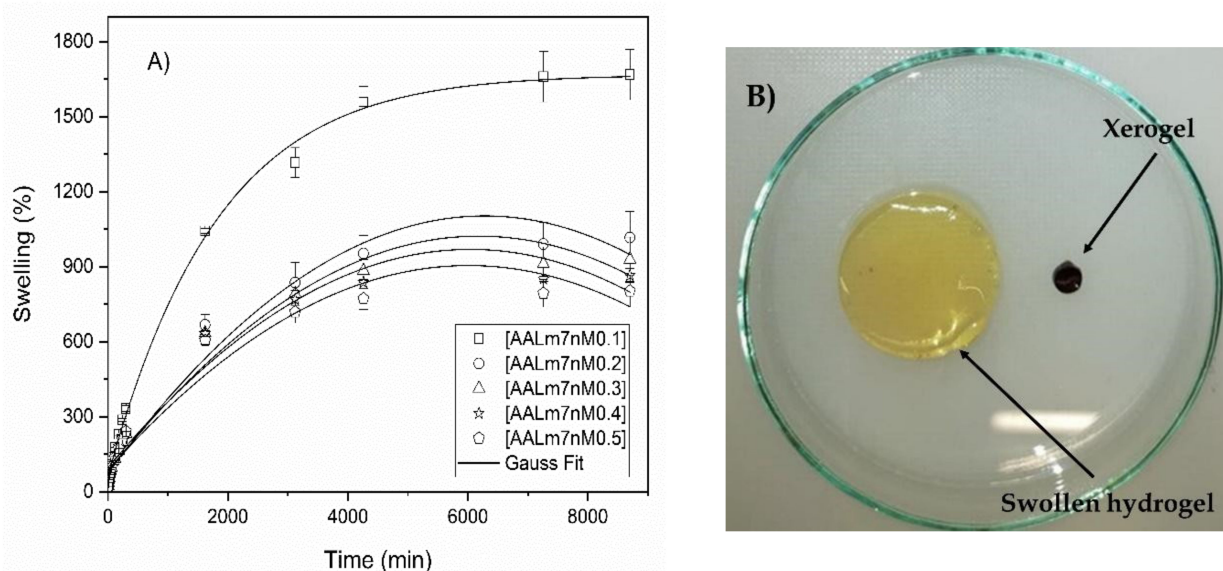


Figure 8. Swelling in water of hydrogels with AA, functionalized AKL and NMBA. (A) Swelling behavior of hydrogels, (B) comparative capture of xerogel and swollen hydrogel.

The incorporation of NMBA in these formulations causes a rigidity in the hydrogel network, hardening it and significantly hindering the passage of water through the structure of these hydrogels. This limits their interaction with water considerably, which causes

the time to reach the maximum swelling percentage to be less than the time required in formulations with only functionalized AKL.

3.2.4. Metal Ions Adsorption Experiments

Figure 9 shows the behavior of the AALm7 and AALm7nM0.1 samples of the synthesized hydrogels (with and without crosslinking agent NMBA).

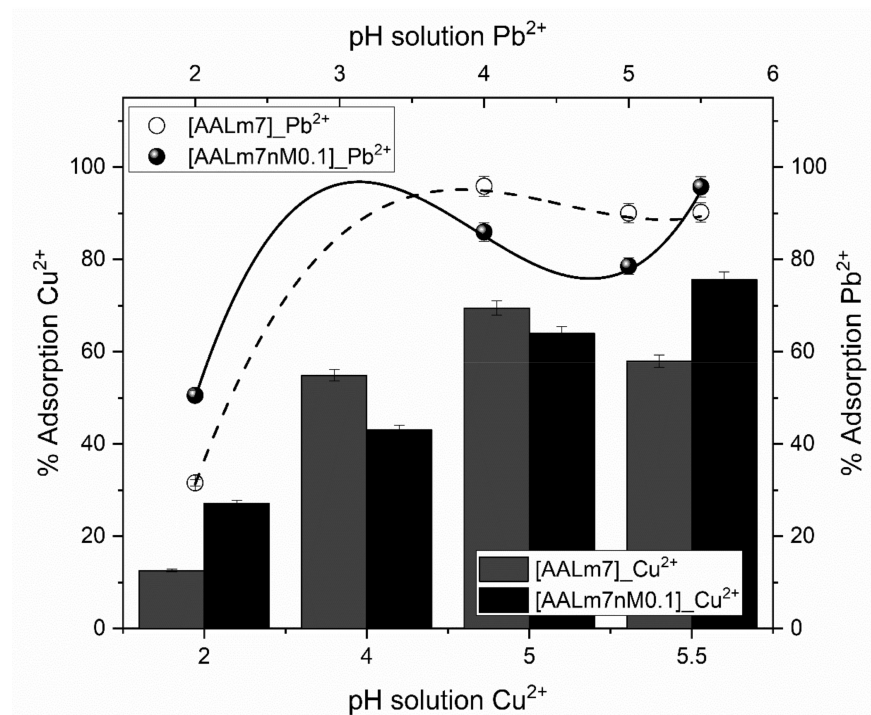


Figure 9. Removal percentage of Pb²⁺ and Cu²⁺ at different pH of the samples AALm7 and AALm7nM0.1.

As can be appreciated these samples were selected due to their excellent swelling capacity to compare the effect of the NMBA in the sorption capacity for Cu²⁺ and Pb²⁺ at different pH values. In this regard, we can observe that in case of the Cu²⁺ adsorption probes in all cases the inclusion of NMBA produces higher adsorption percentages values against the samples without it, this can be attributed in first place to the deprotonation of the functional groups provided by the Acrylic Acid in which higher pH values than 4.7, which corresponds with the pKa of the AA subserves the deprotonation phenomena of the COOH functional group [40], in second place the addition of NMBA to the polymer network provides major rigidity that approaches the functional groups into the hydrogel network who produces higher repulsion charges between functional groups when there are deprotonated due to the negative charges generated for this phenomena, this causes that more Cu²⁺ ions are retained in the hydrogel network [41,42]. On the other hand, the adsorption percentages of Pb²⁺ present the same behavior than the Cu²⁺ adsorption probes but with lower increments respect to the samples without NMBA and in the case of pH 4 and 5 a decrease, this can be attributed to the volume of the Pb²⁺ atom which is bigger than Cu²⁺ atom and restricts the capacity to penetrate the hydrogel network.

Many authors have investigated the use of lignin-based hydrogels as adsorbents in water remediation applications, due to their swelling properties and the reactivity of lignin and its counterpart monomers [26].

E.g., Peñaranda and co-workers [29] synthesized an acrylamide-based hydrogel crosslinked with *N,N'*-methylenebisacrylamide in the presence of lignin to create an interpenetrating polymer network (IPN), where they also studied Cu²⁺ and Ni²⁺ adsorption. They found that adsorption of Ni and Cu increased with the increase of pH, determined as

pH 6 the optimum pH for adsorption, however species such as Pb^{2+} and Cu^{2+} are present in wastewaters with $pH < 6$ [43]. In this sense, the synthesized hydrogels presented in this research shows good selectivity and well adsorption capacity at pH 5.5 considering that these materials are covalent crosslinked polymers in comparison with IPN materials.

4. Conclusions

On this work, the chemical modification of the alkali kraft lignin in aqueous solution was carried out by the addition of acryloyl chloride to incorporate a vinyl group into the structure of the AKL. The FTIR, DSC, 1H -NMR and conductivity analyses show the success of the synthetic procedure and the capability of the modified AKL to potentially act as a crosslinking agent due to the demonstration that the vinyl functional group was added correctly to the lignin structure.

For the synthesis of hydrogels, the characterization results from FTIR and DSC show that the polymeric material has been obtained in a correct way. These hydrogels were tested to a first water swelling kinetics procedure and in this test it was ascertained that the lignin was able to work as a crosslinking agent, since the higher the percentage of lignin, the less percentage of swelling was obtained. However, the results of the swelling percentages of the samples with only lignin were lower than the results obtained with samples that have lignin and in addition cross-linked (*N,N*-methylenebisacrylamide).

The metal ions adsorption experiments show the potential application of the hydrogels for the removal of heavy metal ions as a versatile alternative for wastewater treatment.

Author Contributions: Formal analysis, L.G.G.-R., L.R.C.-Z. and E.B.F.-O.; Investigation, D.R.-G.; Methodology, R.A.G.-S., L.P.-A. and J.L.V.-V.; Project administration, S.L.H.-O.; Resources, E.O.-G. All authors have read and agreed to the published version of the manuscript.

Funding: This research received no external funding.

Institutional Review Board Statement: Not applicable.

Informed Consent Statement: Not applicable.

Data Availability Statement: Not applicable.

Acknowledgments: Financial support for this project was provided by the University of Guadalajara through the PROSNI2019 project. Additionally, Diana Rico Garcia thanks the scholarship (736957) granted by the National Council of Science and Technology (CONACYT), Mexico.

Conflicts of Interest: The authors declare no conflict of interest.

References

1. Jeon, C.; Höll, W.H. Application of the surface complexation model to heavy metal sorption equilibria onto aminated chitosan. *Hydrometallurgy* **2004**, *71*, 421–428. [[CrossRef](#)]
2. Rasheed, T.; Bilal, M.; Nabeel, F.; Adeel, M.; Iqbal, M.N. Environmentally-related contaminants of high concern: Potential sources and analytical modalities for detection, quantification, and treatment. *Environ. Int.* **2019**, *122*, 52–66. [[CrossRef](#)] [[PubMed](#)]
3. Sengupta, A.K.; Zhu, Y.; Hauze, D. Metal(II) ion binding onto chelating exchangers with nitrogen donor atoms: Some new observations and related implications. *Environ. Sci. Technol.* **1991**, *25*, 481–488. [[CrossRef](#)]
4. Chao, A. Enzymatic grafting of carboxyl groups on to chitosan—to confer on chitosan the property of a cationic dye adsorbent. *Bioresour. Technol.* **2004**, *91*, 157–162. [[CrossRef](#)]
5. Kaşgöz, H.; Kaşgöz, A.; Şahin, Ü.; Temelli, T.Y.; Bayat, C. Hydrogels with Acid Groups for Removal of Copper(II) and Lead(II) Ions. *Polym. Technol. Eng.* **2006**, *45*, 117–124. [[CrossRef](#)]
6. Li, N.; Bai, R. A Novel Amine-Shielded Surface Cross-Linking of Chitosan Hydrogel Beads for Enhanced Metal Adsorption Performance. *Ind. Eng. Chem. Res.* **2005**, *44*, 6692–6700. [[CrossRef](#)]
7. Chauhan, G.S.; Chauhan, K.; Chauhan, S.; Kumar, S.; Kumari, A. Functionalization of pine needles by carboxymethylation and network formation for use as supports in the adsorption of Cr^{6+} . *Carbohydr. Polym.* **2007**, *70*, 415–421. [[CrossRef](#)]
8. Çavuş, S.; Gürdağ, G. Noncompetitive Removal of Heavy Metal Ions from Aqueous Solutions by Poly[2-(acrylamido)-2-methyl-1-propanesulfonic acid-co-itaconic acid] Hydrogel. *Ind. Eng. Chem. Res.* **2009**, *48*, 2652–2658. [[CrossRef](#)]
9. Katime, I.; Rodriguez, E. Absorption of metal ions and swelling properties of poly(acrylic acid-co-itaconic acid) hydrogels. *J. Macromol. Sci. Part A* **2001**, *38*, 543–558. [[CrossRef](#)]

10. Kofinas, P.; Kioussis, D.R. Reactive Phosphorus Removal from Aquaculture and Poultry Productions Systems Using Polymeric Hydrogels. *Environ. Sci. Technol.* **2002**, *37*, 423–427. [[CrossRef](#)]
11. Gandini, A.; Belgacem, M.N. Lignins as Components of Macromolecular Materials. *Monomers Polym. Compos. Renew. Resour.* **2008**, 243–247. [[CrossRef](#)]
12. Datta, R.; Kelkar, A.; Baraniya, D.; Molaei, A.; Moulick, A.; Meena, R.S.; Formanek, P. Enzymatic Degradation of Lignin in Soil: A Review. *Sustainability* **2017**, *9*, 1163. [[CrossRef](#)]
13. Leonowicz, A.; Matuszewska, A.; Luterek, J.; Ziegenhagen, D.; Wojtas-Wasilewska, M.; Cho, N.S.; Hofrichter, M.; Rogalski, J. Review Biodegradation of Lignin by White Rot Fungi. *Fungal Genet. Biol.* **1999**, *27*, 175–185. [[CrossRef](#)] [[PubMed](#)]
14. Figueiredo, P.; Lintinen, K.; Hirvonen, J.T.; Kostianen, M.A.; Santos, H.A. Properties and chemical modifications of lignin: Towards lignin-based nanomaterials for biomedical applications. *Prog. Mater. Sci.* **2018**, *93*, 233–269. [[CrossRef](#)]
15. Muzzarelli, R.A. Genipin-crosslinked chitosan hydrogels as biomedical and pharmaceutical aids. *Carbohydr. Polym.* **2009**, *77*, 1–9. [[CrossRef](#)]
16. Demitri, C.; Del Sole, R.; Scalera, F.; Sannino, A.; Vasapollo, G.; Maffezzoli, A.; Ambrosio, L.; Nicolais, L. Novel superabsorbent cellulose-based hydrogels crosslinked with citric acid. *J. Appl. Polym. Sci.* **2008**, *110*, 2453–2460. [[CrossRef](#)]
17. Chen, X.; Li, P.; Kang, Y.; Zeng, X.; Xie, Y.; Zhang, Y.; Wang, Y.; Xie, T. Preparation of temperature-sensitive Xanthan/NIPA hydrogel using citric acid as crosslinking agent for bisphenol A adsorption. *Carbohydr. Polym.* **2019**, *206*, 94–101. [[CrossRef](#)]
18. Korey, M.; Mendis, G.P.; Youngblood, J.P.; Howarter, J.A. Tannic acid: A sustainable crosslinking agent for high glass transition epoxy materials. *J. Polym. Sci. Part A Polym. Chem.* **2018**, *56*, 1468–1480. [[CrossRef](#)]
19. Liang, H.-C.; Chang, W.-H.; Liang, H.-F.; Lee, M.-H.; Sung, H.-W. Crosslinking structures of gelatin hydrogels crosslinked with genipin or a water-soluble carbodiimide. *J. Appl. Polym. Sci.* **2004**, *91*, 4017–4026. [[CrossRef](#)]
20. Hoffman, A.S. Hydrogels for biomedical applications. *Adv. Drug Deliv. Rev.* **2012**, *64*, 18–23. [[CrossRef](#)]
21. Meng, Y.; Lu, J.; Cheng, Y.; Li, Q.; Wang, H. Lignin-based hydrogels: A review of preparation, properties, and application. *Int. J. Biol. Macromol.* **2019**, *135*, 1006–1019. [[CrossRef](#)] [[PubMed](#)]
22. Singhal, R.; Gupta, K. A Review: Tailor-made Hydrogel Structures (Classifications and Synthesis Parameters). *Polym. Technol. Eng.* **2015**, *55*, 54–70. [[CrossRef](#)]
23. Zheng, S.; Li, Z.; Liu, Z. The fast homogeneous diffusion of hydrogel under different stimuli. *Int. J. Mech. Sci.* **2018**, *137*, 263–270. [[CrossRef](#)]
24. Richter, A.; Paschew, G.; Klatt, S.; Lienig, J.; Arndt, K.-F.; Adler, H.-J.P. Review on Hydrogel-based pH Sensors and Microsensors. *Sensors* **2008**, *8*, 561. [[CrossRef](#)] [[PubMed](#)]
25. Jeong, B.; Kim, S.W.; Bae, Y.H. Thermosensitive sol–gel reversible hydrogels. *Adv. Drug Deliv. Rev.* **2012**, *64*, 154–162. [[CrossRef](#)]
26. Rico-garc, D.; Ruiz-rubio, L.; Leyre, P. Lignin-Based Hydrogels: Synthesis and Applications. *Polymers* **2020**, *12*, 81. [[CrossRef](#)] [[PubMed](#)]
27. Xue, W.; Hamley, I.W.; Huglin, M.B. Rapid swelling and deswelling of thermoreversible hydrophobically modified poly(N-isopropylacrylamide) hydrogels prepared by freezing polymerisation. *Polymer* **2002**, *43*, 5181–5186. [[CrossRef](#)]
28. Sun, X.-F.; Zeng, Q.; Wang, H.; Hao, Y. Preparation and swelling behavior of pH/temperature responsive semi-IPN hydrogel based on carboxymethyl xylan and poly(N-isopropyl acrylamide). *Cellulose* **2018**, *26*, 1909–1922. [[CrossRef](#)]
29. Sabino, M.A. Effect of the presence of lignin or peat in IPN hydrogels on the sorption of heavy metals. *Polym. Bull.* **2010**, *65*, 495–508. [[CrossRef](#)]
30. Feng, Q.; Chen, F.; Zhou, X. Preparation of Thermo-Sensitive Hydrogels from Acrylated Lignin and N-Isopropylacrylamide Through Photocrosslinking. *J. Biobased Mater. Bioenergy* **2012**, *6*, 336–342. [[CrossRef](#)]
31. Brannigan, R.P.; Khutoryanskiy, V.V. Synthesis and evaluation of mucoadhesive acryloyl-quaternized PDMAEMA nanogels for ocular drug delivery. *Colloids Surfaces B Biointerfaces* **2017**, *155*, 538–543. [[CrossRef](#)]
32. Yang, P.; Li, D.; Jin, S.; Ding, J.; Guo, J.; Shi, W.; Wang, C. Stimuli-responsive biodegradable poly(methacrylic acid) based nanocapsules for ultrasound traced and triggered drug delivery system. *Biomaterials* **2014**, *35*, 2079–2088. [[CrossRef](#)] [[PubMed](#)]
33. Ding, L.; Li, Y.; Jia, D.; Deng, J.; Yang, W. β -Cyclodextrin-based oil-absorbents: Preparation, high oil absorbency and reusability. *Carbohydr. Polym.* **2011**, *83*, 1990–1996. [[CrossRef](#)]
34. An, Y.-X.; Li, N.; Wu, H.; Lou, W.-Y.; Zong, M.-H. Changes in the Structure and the Thermal Properties of Kraft Lignin during Its Dissolution in Cholinium Ionic Liquids. *ACS Sustain. Chem. Eng.* **2015**, *3*, 2951–2958. [[CrossRef](#)]
35. Glasser, W.G. Classification of Lignin According to Chemical and Molecular Structure. *Monomers Polym. Compos. Renew. Resour.* **2000**, *742*, 216–238.
36. Lora, J.H.; Glasser, W.G. Recent Industrial Applications of Lignin: A Sustainable Alternative to Nonrenewable Materials. *J. Polym. Environ.* **2002**, *10*, 39–48. [[CrossRef](#)]
37. Ji, X.; Zhang, Z.; Chen, J.; Yang, G.; Lucia, L.A. Synthesis and Characterization of Alkali Lignin-based Hydrogels from Ionic Liquids. *BioResources* **2017**, *12*, 5395–5406. [[CrossRef](#)]
38. Callemant, C.J. The metabolism and pharmacokinetics of acrylamide: Implications for mechanisms of toxicity and human risk estimation. *Drug Metab. Rev.* **1996**, *28*, 527–590. [[CrossRef](#)]
39. Domínguez-Robles, J.; Peresin, M.S.; Tamminen, T.; Rodríguez, A.; Larrañeta, E.; Jääskeläinen, A.-S. Lignin-based hydrogels with “super-swelling” capacities for dye removal. *Int. J. Biol. Macromol.* **2018**, *115*, 1249–1259. [[CrossRef](#)]

40. Betancourt, T.; Pardo, J.; Soo, K.; Peppas, N.A. Characterization of pH-Responsive Hydrogels of Poly(Itaconic acid-g-Ethylene Glycol) Prepared by UV-Initiated Free Radical Polymerization as Biomaterials for Oral Delivery of Bioactive Agents. *J. Biomed. Mater. Res.* **2011**, *93*, 175–188. [[CrossRef](#)]
41. Lange, H.; Decina, S.; Crestini, C. Oxidative upgrade of lignin—Recent routes reviewed. *Eur. Polym. J.* **2013**, *49*, 1151–1173. [[CrossRef](#)]
42. Rizwan, M.; Yahya, R.; Hassan, A.; Yar, M.; Azzahari, A.D.; Selvanathan, V.; Sonsudin, F.; Abouloula, C.N. pH Sensitive Hydrogels in Drug Delivery: Brief History, Properties, Swelling, and Release Mechanism, Material Selection and Applications. *Polymers* **2017**, *9*, 137. [[CrossRef](#)] [[PubMed](#)]
43. Çelebi, H.; Gök, G.; Gök, O. Adsorption capability of brewed tea waste in waters containing toxic lead(II), cadmium (II), nickel (II), and zinc(II) heavy metal ions. *Sci. Rep.* **2020**, *10*, 17570. [[CrossRef](#)] [[PubMed](#)]